Malaysian Journal of Analytical Sciences (MJAS)



Published by Malaysian Analytical Sciences Society

ANALYTICAL COMPARATIVE STUDIES OF ADSORPTION EFFICIENCY OF MCM-41 AND SBA-15 ON REMOVAL OF ANIONIC-AZO AND CATIONIC DYES FROM AQUEOUS SAMPLE

(Kajian Perbandingan Analisis Keberkesanan Penjerapan MCM-41 dan SBA-15 untuk Penyingkiran Pewarna Anionik-Azo dan Kationik Dari Sampel Akueus)

Nur Zabirah Zabi¹, Wan Nazihah Wan Ibrahim^{1*}, Nur Husna Zainal Abidin¹, Siti Syairah Mat Salleh¹, Farah Amira Shahrul Effendi¹, Isna Fazliana Mohamed Idrus¹, Hamizah Md Rasid¹, Nursyamsyila Mat Hadzir¹, Nor Suhaila Mohamad Hanapi¹, Mazhani Muhammad²

 ¹ School of Chemistry and Environment, Faculty of Applied Sciences, Universiti Teknologi MARA, 40450 Shah Alam, Selangor, Malaysia
 ² Centre of Foundation Studies (CFS),
 Universiti Teknologi MARA, 438000 Dengkil Campus, Selangor, Malaysia

*Corresponding author: wannazihah@uitm.edu.my

corresponding dunor. wantaguan e unincau.my

Received: 29 June 2021; Accepted: 15 August 2021; Published: xx October 2021

Abstract

Mobil Composition of Matter No. 41 (MCM-41) and Santa Barbara Amorphous (SBA-15), a type of mesoporous adsorbents, were successfully prepared via mixed cationic-neutral templating route and sol-gel method, respectively. Analytically, the prepared materials were compared to remove anionic azo (methyl orange) and cationic dyes (methylene blue) from highly colored solutions. Both adsorbents were characterized using Fourier transform infrared (FTIR), field emission scanning electron microscopy (FESEM), and nitrogen adsorption/desorption to enhance the understanding of structure and surface properties. To assess the efficiency of the prepared adsorbents, the pH of the sample, the initial concentration of the dyes, and contact time were studied. At optimum conditions, maximum adsorption capacities for methyl orange (MO) and methylene blue (MB) using MCM-41 were 4.757 mg/g and 16.00 mg/g and for SBA-15 the maximum adsorption capacities were 20.212 mg/g and 10.45 mg/g, respectively. Furthermore, Langmuir and Freundlich isotherm models were selected to describe the adsorption process while pseudo-first-order and pseudo-second-order kinetics equations were applied to determine the adsorption kinetics. The obtained results showed that SBA-15 can remove both dyes 38.53% better than MCM-41 due to higher surface area, which was 507 m²/g compared to 436 m²/g for MCM-41.

Keywords: cationic dyes, anionic dyes, adsorption, mesoporous silica

Abstrak

Komposisi Mobil Perkara 41 (MCM-41) dan Santa Barbara Amorfous (SBA-15) jenis penjerap mesopori berjaya disediakan melalui kaedah templat neutral kationik-neutral dan kaedah sol-gel. Bahan yang disediakan dibandingkan secara analitikal untuk mengeluarkan pewarna azo anionik (oren metil) dan pewarna kationik (biru metilena) dari larutan yang sangat berwarna. Kedua-dua penjerap dicirikan menggunakan inframerah jelmaan Fourier (FTIR), mikroskopi elektron pengimbasan pelepasan medan

(FESEM) dan penjerapan/penyahjerapan nitrogen untuk meningkatkan pemahaman mengenai sifat struktur dan permukaan. Untuk menilai kecekapan penjerap yang telah disediakan, tiga parameter telah dikaji iaitu pH sampel, kepekatan awal pewarna dan masa penyentuhan. Pada keadaan optimum, kapasiti penjerapan maksimum untuk metil oren (MO) dan metilena biru (MB) menggunakan MCM-41 ialah 4.757 mg/g dan 16.00 mg/g dan untuk SBA-15 kapasiti penjerapan maksimum ialah 20.212 mg/g dan 10.45 mg/g masing-masing. Selanjutnya, model isoterm Langmuir dan Freundlich dipilih untuk menggambarkan proses penjerapan sementara persamaan kinetik turutan-pseudo-pertama dan turutan-pseudo-kedua digunakan untuk menentukan kinetik penjerapan. Hasil perolehan menunjukkan bahawa SBA-15 dapat menyerap kedua-dua pewarna 38.53% lebih baik daripada MCM-41 kerana luas permukaannya yang lebih tinggi iaitu 507 m²/g berbanding dengan 436 m²/g untuk MCM-41.

Kata kunci: pewarna kation, pewarna anion, penjerapan, silika mesopori

Introduction

Dye molecules contain chromophore and auxochrome structures. Chromophore group contains a double bond that oscillates to absorb light and causes a dye to have a visible colour [1]. Natural dyes gave dull colors and were commonly used in the European textile industry before synthetic dyes were produced in 1856 [2]. Dyes are widely used in foods, medicines, and clothes resulting in an increase in dye production [3]. Acid dyes, basic dyes, direct dyes, disperse dyes, reactive dyes and vat dyes are commonly used in textile industrial products [4]. MO is an example of acid or anionic dye that belongs to azo dye which consists of one or more azo groups (-N=N-) between the carbons [5, 6]. Azo dyes are also commonly used in food and could cause bladder cancer when consumed, due to the presence of benzidine, a known carcinogenic agent [7, 8] MB is a basic or cationic dye with a structure of heterocyclic aromatic chemical compound [9]. MB can cause a burning sensation leading to permament injury when in contact with the eyes [10]. In addition to the health effect, the environment could also be affected by the pollution of dyes as this water-soluble compound cannot be easily removed through a filtration method. As a result, it can affect the symbiotic process due to the prevention of light penetration, which leads to low photosynthetic activity in the water [11]. Besides that, a large number of synthetic dyes are released into wastewater during coloration process due to illegal and improper waste management [3].

Various techniques have been developed to remove dye from water including nanofiltration [12], electrochemical coagulation [13], reverse osmosis [14], photochemical degradation [15], ion exchange [16] and

adsorption. However, adsorption is more beneficial compared to other techniques due to the simplicity of design, case of operation, initial cost, and insensitivity to toxic substances [17]. The efficiency of the adsorption technique is based on the adsorbent properties, which are high adsorption capacity and selectivity, good mechanical stability, resource abundance, and environmental friendly [18]. Therefore, scientists have developed various kinds of adsorbent from coffee wastes [5], banana plant-derived sorbents [19], calcined and uncalcined Mg/Al layered double hydroxide [20], cellulose-based porous adsorbents [21], activated carbons [22, 23], magnetic lignin-based adsorbent [24], anionic clay-layered double hydroxide [25], amino-cross linked hypromellose [26], and double hydroxide/polyacrylamide layered nanocomposite hydrogels [27] to increase the efficiency of removing a dye. Nonetheless, these types of adsorbents may have their drawbacks such as, expensive to synthesize, difficult to dispose, low adsorption efficiency or difficult, and costly to regenerate [28, 29]. The discovery of mesoporous silica has garnered a lot of attention from researchers since it has high surface areas and well-defined pore structures [30]. The first mesoporous material was created through hydrothermal reaction using aluminisilicate gel with the presence of surfactants [31].

Mobil Composition of Matter No. 41 (MCM-41) and Santa Barbara Amorphous (SBA-15) are a member of the mesoporous family and are suitable for dye removal due to their high specific surface area ranging from 500 to 1000 m²/g [32]. The pore sizes of SBA-15 and MCM-41 are in the range of 60 to 110 Å and 15 to 100 Å, respectively [33, 34]. Furthermore, the hydroxyl

group (-OH) on their surface area offer ease functionalization to enhance their selectivity [33, 35, 36]. These two adsorbents are preferable compared to other adsorbents because the surface and pores of these materials can be altered to target specific analytes, regenerated, and reused with high capacity at low cost [29]. The objectives of this study are to prepare and characterize mesoporous silica MCM-41 via mixed cationic-neutral templating route using cationic cetyl trimethylammonium bromide and SBA-15 via sol-gel method. This is performed; to assess the performance of prepared adsorbent for removal of anionic MO and cationic MB dyes using ultraviolet -visible spectroscopy.

Materials and methods

Chemicals and reagents

The chemicals that were used in this study are cetyltrimethylammonium bromide (CTABr, 99%, Sigma-Aldrich), 1.0 M aqueous hydroxide (NaOH, Sigma-Aldrich) and Ludox colloidal silica (SiO₂, 30%, Sigma-Aldrich), ammonium hydroxide (NH₄OH, 25%), MB ($C_{16}H_{18}C_1N_3S$, 90%, Sigma-Aldrich), MO ($C_{14}H_{14}N_3NaO_3S$, 90%, Sigma-Aldrich), and distilled water.

Preparation of MCM-41 and SBA-15

The method used to synthesize MCM-41 was adapted with slight modification from a previous study [37]. Sodium silicate (solution A) was firstly prepared by mixing 33.80 mL of Ludox (30%) with 3.03 g of sodium hydroxide (NaOH) in 37.5 mL double distilled water at 80 °C with 2 hours stirring at a medium speed using magnetic stirrer. Then, another solution (solution B) was separately prepared by mixing 9.60 g of cetyltrimethylammonium bromide (CTABr) and 0.50 g of ammonium hydroxide (NH4OH) in 75.0 mL of distilled water with stirring at 80 °C until a clear solution was obtained. Both A and B solutions were mixed in a polypropylene bottle to give a gel with a composition of 6 SiO₂: CTABr: 1.5 Na₂O: 0.15 (NH₄)₂O: 250H₂O followed with vigorous stirring. The resulting gel was then kept in an oven for crystallization at 100 °C for 24 hours. The following day, the gel was then cooled to room temperature for 3 hours, and the pH was adjusted to 10.2 by adding 25

wt.% of acetic acid. The heating and pH adjustments were repeated twice in order to complete the polymerization process of silica monomers. The white conducts were filtered, washed, neutralized, and dried overnight at 100 °C in an electrical oven. Finally, the solid product went through a calcination process at 550 °C in a furnace for 10 hours to remove the organic template.

The preparation of SBA-15 was referred to previous study with minor modifications [38]. Firstly, distillate water (30 mL), 2.0 M HCl (120 mL), and Pluronic P123 (4.0 g) were dissolved by stirring at 35 °C for 20 hours. Then, 8.5 g of tetraethyl-orthosilicate (TEOS) was added dropwise under constant vigorous stirring for 15 minutes. The mixture was kept under static conditions at 35 °C for 20 hours. The milky mixture was then placed in an oven at 90 °C for 24 hours. The solid product was filtered, washed, and dried at 45 °C for 72 hours. Lastly, the product was calcined for 6 hours at 500 °C and stored in a proper container.

Characterization of MCM-41 and SBA-15

The functional groups that are present in both adsorbents were determined using FTIR (Perkin Elmer 8300, Massachusetts, USA). Each adsorbent was ground with KBr powder to turn it into a pellet before obtaining the FTIR spectrum. The surface morphology of both adsorbents was identified using FESEM (JEOL JEM-2300, Tokyo, Japan) after it was coated with gold film at 20kV voltage. In addition, the specific surface area and averaged pore size were analyzed using Brunauer-Emmett-Teller (BET) surface analyser (Belsorp-mini II, Japan). The samples were displaced at 300 °C with nitrogen flow for 6 hours. The surface area of each adsorbent was discovered from the linear BET method with rapid nitrogen uptake, P/P₀ = (0.4-1.0).

Batch studies on MO and MB removal

The batch studies were carried out to investigate the adsorption reaction of MO and MB onto MCM-41 and SBA-15 by varying the pH values of the sample, the initial concentration of both dyes, and contact time. Each parameter gave an effect on the adsorption capacity of the dyes using MCM-41 and SBA-15 as the

adsorbent. The adsorbent dosage was kept constant at 0.05 g. The removal process was obtained by placing a conical flask containing dye solution (10 mL) and 0.05 g adsorbent onto a shaker with a constant speed at 160 rpm. The adsorbent was separated from the dye solution through centrifugation. The residual MO and MB concentrations were then determined by collecting aliquots from the supernatant and measuring them with a UV-Vis spectrophotometer (Lambda 35-Perkin Elmer) at a wavelength of 463 nm for MO and 660 nm for MB [39].

Adsorption isotherm

Adsorption equilibrium provides the fundamental physicochemical data to evaluate the applicability of the adsorption process [40]. The adsorption data of the experiment were fitted according to the two isotherm models, which were Langmuir and Freundlich models. Langmuir model predicts that each adsorbate molecule is located at a single site of identical energy onto the surface of the adsorbent that leads to a formation of a monolayer [41]. The equation for this model is presented in Equation (1).

$$\frac{c_e}{q_e} = \frac{1}{Q_{mb}} + \frac{c_e}{Q_m} \tag{1}$$

where C_e is equilibrium concentration of adsorbate, q_e is amount of dye adsorbed (mg/g), Q_m = adsorption capacity (mg/g), and b is Langmuir constant (L/mg) which were determined through intercept value from $\frac{c_e}{q_e}$ against C_e graph.

Freundlich model is an empirical equation utilized to define equilibrium on heterogenous surfaces and hence does not assume monolayer capacity [42]. The equation used to represent this model is stated in Equation (2).

$$\log q_e = \log K_f + \frac{1}{n} \log C_e \tag{2}$$

where k_f is adsorption capacity, n is Freundlich constant, C_e is equilibrium concentration of adsorbate, q_e is capacity of equilibrium adsorption and n were determined from the intercept and slope of graph $ln(q_e)$ against $ln(C_e)$.

Adsorption kinetics

The experimental data were fitted by implementing pseudo-first-order and pseudo-second-order kinetic models [41]. The equation for pseudo-first-order and pseudo-second-order is stated in Equation (3) and (4), respectively.

$$\log_{10}(q_e - q_t) = \log_{10}(q_e) - \frac{k_1}{2.303}$$
 (3)

where q_t is amount of dye adsorbs at certain time equilibrium, k_1 is equilibrium rate constant of pseudo-first constant and $t = time \, (min)$.

$$\frac{t}{q_t} = \frac{1}{k_2 q_e^2} + \frac{t}{q_e} \tag{4}$$

where K_2 is pseudo-second-order rate constant, q_e is capacity of equilibrium adsorption, q_t is adsorption amount of dye at certain time equilibrium, t is contact time (min), q_e and K_2 were calculated using $\frac{t}{q_t}$ against t graph.

Results and Discussion

Characterization of MCM-41 and SBA-15

FTIR-ATR spectra of MCM-41 and SBA-15 are shown in Figure 1. The broad peak around 3500 and 1639 cm⁻ 1 in both spectra are mainly due to the bending vibration of the adsorbed water. The bands present around 1030 - 1080 and 450 - 464 cm⁻¹ indicate siloxane bond (Si-O-Si) and Si-O bond in both samples, respectively. The peaks representing silanol group (Si-OH) in MCM-41 and SBA-15 are present around 800 - 970 cm⁻¹ [43, 44, 45, 47, 48]. These four bonds confirm the silica framework of MCM-41 and SBA-15 [45]. However, SBA-15 contains two extra bonds, which are stretching vibration of C=O (the peak is present at 1701 cm⁻¹) and C-H bending (the peak is present at 1370 cm⁻¹) [45, 46]. Both adsorbents have similar bonds but there are slight differences in their wavenumbers.

FESEM micrographs of both adsorbents are shown in Figure 2. The morphology of each adsorbent is different. On the surface of MCM-41, the presence of pores could be observed after the removal of the CTABr template and the shape appeared as small

agglomerated spheres and small rods [49]. SBA-15 shows a perfect sphere due to the removal of triblock copolymer surfactant [50].

The specific surface area, pore volume and pore diameter parameters of the synthesized materials were calculated using the BET method based on the N_2 adsorption and desorption isotherms. N_2 adsorption/desorption isotherms of MCM-41 and SBA-15 are shown in Figure 3. According to the International Union of Pure and Applied Chemistry (IUPAC), the isotherms of both MCM-41 and SBA-15

exhibit typical type IV physisorption curves thus, confirming that both adsorbents are mesoporous and the adsorption process can either be monolayer or multilayer [51]. As for the type of hysteresis loop, both adsorbents show type H1 that often relate to porous materials with well-defined cylindrical-like pore channels or agglomerates of approximately uniform spheres [34]. The specific surface area, pore volume, and pore diameter for MCM-41 are 436 m²/g, 0.533 cm³/g and 11.27 nm while for SBA-15 are 507 m²/g, 0.688 cm³/g and 7.2 nm, respectively.

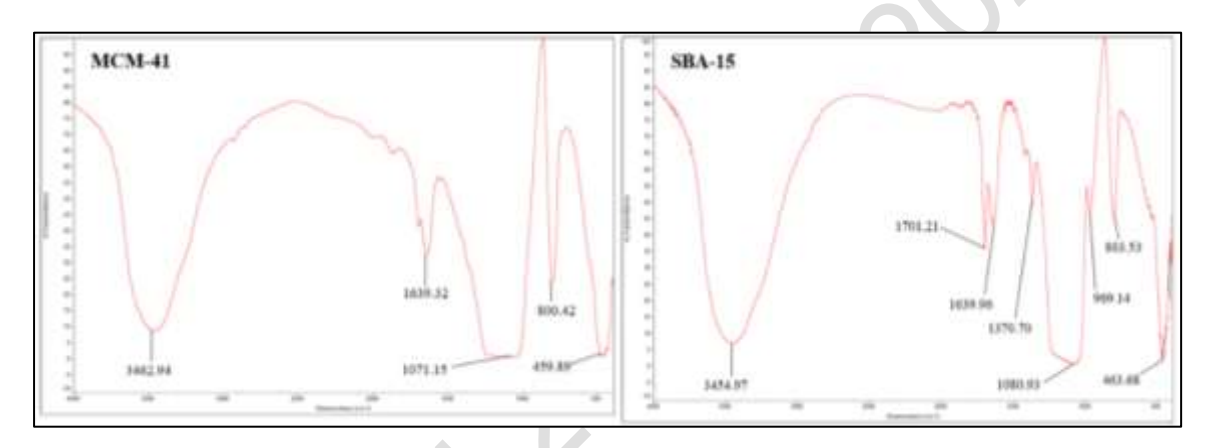


Figure 1. FTIR spectra of (a) MCM-41 and (b) SBA-15

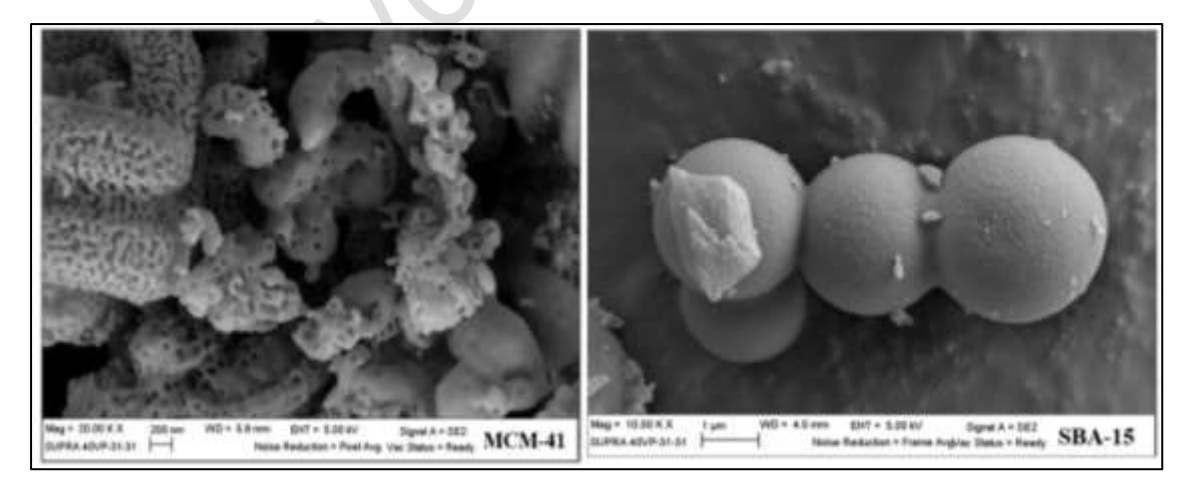


Figure 2. FESEM micrographs of (a) MCM-41 and (b) SBA-15

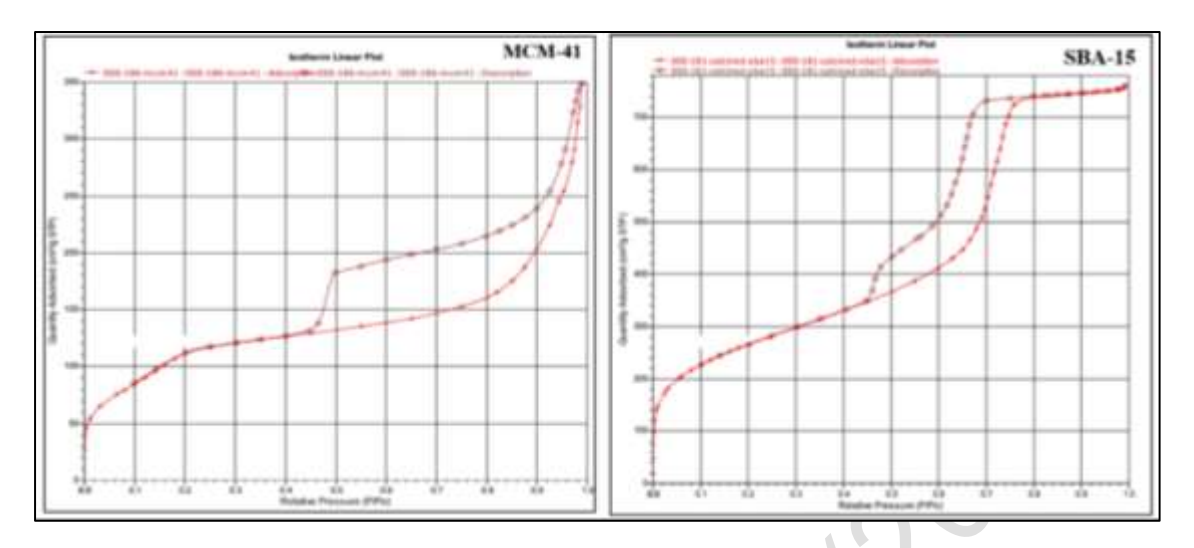


Figure 3. N₂ Adsorption-Desorption Isotherms of MCM-41 and SBA-15

Batch adsorption studies of MO and MB using calcined MCM-41 and SBA-15

Effect of sample pH

The pH of the sample affects every adsorption process especially for dyes since pH controls the magnitude of electrostatic charges on the surface of the adsorbent. When optimized pH is obtained, the adsorbent can adsorb more dye molecules since the surface of the adsorbent have the suitable electrostatic charge to interact with the anionic and cationic dye molecules that have negative and positive charge once the dyes dissolved and partially ionized in water [52]. To study the effect of pH (3, 5, 7, 9, and 11), the pH of the dye solution was adjusted in a beaker before being transferred to a conical flask. In this experiment, 0.01 M NaOH, 0.1 M NaOH, 0.01 M HCl, and 0.1 M HCl was used to adjust the pH systematically. The other variables were set at constant values including sample volume (10 mL), the mass of adsorbent (0.05 g), shaker speed (160 rpm), dye concentration (80 ppm), and contact time (30 mins).

Figure 4, shows that the optimum pH for removal of MO using MCM-41 is pH 3 while SBA-15 is pH 5 with a percentage removal of 58% (MCM-41) and 55.17% (SBA-15). Under an acidic condition, there is a high concentration of H⁺ that will change the surface of the adsorbents to be slightly positively charged and

increase its ability to adsorb MO that has a negative charge once it dissolves in water [53]. For removal of MB, the optimum pH using MCM-41 and SBA-15 are pH 7 and pH 11, respectively with a percentage removal of 100.24% (MCM-41) and 99.95% (SBA-15). Cationic dyes such as MB gives positively charged ions when dissolved in water and due to this acidic medium (pH<7), the surface of the adsorbent becomes positively charged and tends to oppose the adsorption of the MB molecules. At higher pH (pH \geq 7), the electrostatic repulsion between the positively charged MB and the surface of the adsorbent was lowered since there were less H⁺ ions to compete with cation groups on dye for adsorption sites hence, increasing the removal efficiency of the dye molecules [54-56]. Another study, stated that increasing the pH of the sample will increase the number of hydroxyl (OH-) ions thus, increasing the number of negatively charged sites on the surface of the adsorbent and enlarges the attraction between MB and adsorbent surface [57] Based on the percentage removal, both MCM-41 and SBA-15 adsorbed more MB compared to MO. This might be due to the presence of silanol groups that have acidic character and are able to form hydrogen bonds with MB molecules compared to MO molecules [30]. It was also found that there is a slight difference in percentage removal of MB between these two adsorbents. However, both adsorbents are still

considered efficient adsorbents [39]. Figure 5 shows the adsorption mechanism under basic and acidic conditions. Based on Figure 5, it shows that the silanol group on the surface of the adsorbents interacts with the dye molecules. In an acidic condition, the silanol groups become slightly positive when it reacts with H⁺

ions and become Si-OH₂⁺ that enable the adsorbents to adsorb the MO molecules and in basic condition, the silanol groups become slightly negative when OH⁻ ions react with the group and become Si-O⁻ and enable the adsorbents to adsorb MB molecules [53].

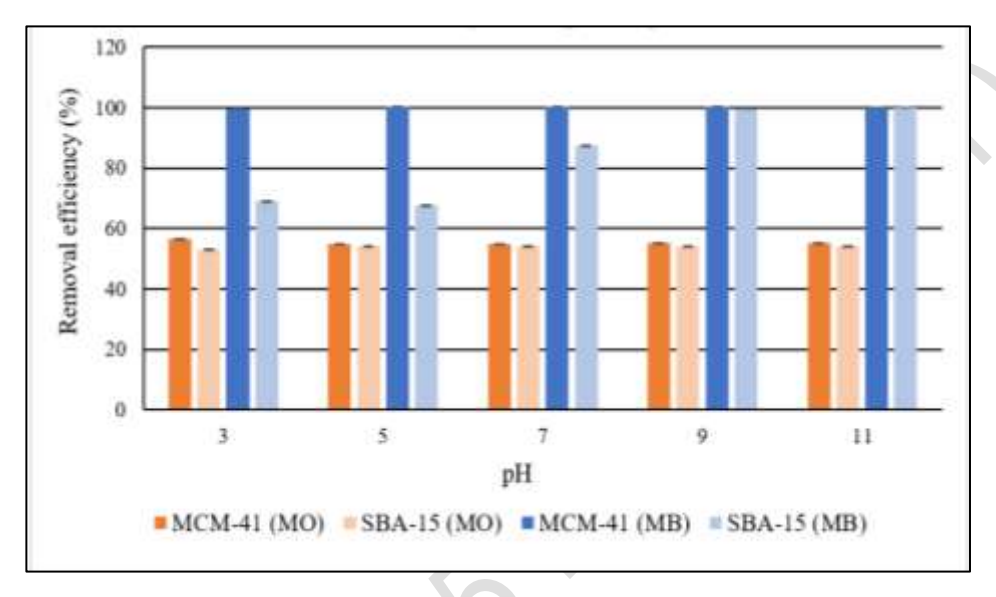


Figure 4. Percentage removal of MO and MB using MCM-41 and SBA-15 at a different range of pH

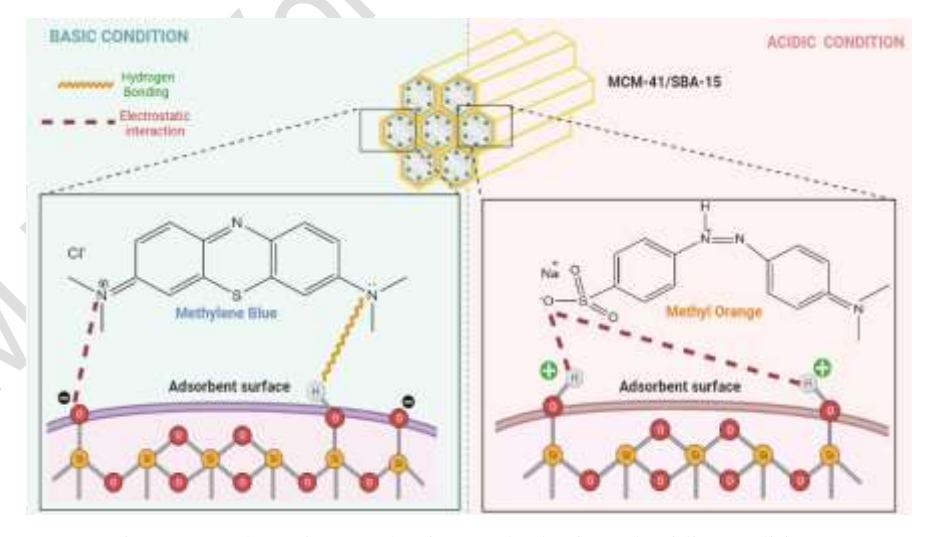


Figure 5. Adsorption mechanism under basic and acidic conditions

Effect of initial concentration

The study on the initial concentration of MO and MB was carried out to determine the adsorption capacity of each adsorbent. The initial concentration used was 60 ppm, 80 ppm, 100 ppm, 120 ppm, and 140 ppm with an adsorbent dosage of 0.05 g. For MCM-41, the pH value of MO solution was set to 3 with a contact time of 30 minutes while for MB, the pH was set to pH 9 with the same contact time. As for SBA-15, the pH value of the MO solution was set to pH 5 with a contact time of 30 minutes while for MB, the pH was set to pH 7 with the same contact time. The initial concentration of the dye will affect the amount of adsorption for dye removal. The amount of dye adsorbed onto the adsorbent is highly dependant on the available sites of the adsorbent surface. As seen in Figure 6, the optimum initial concentration for removal of MO using MCM-41 and SBA-15 is 60 ppm and 140 ppm respectively with a percentage removal of 100% (MCM-41) and 72.54% (SBA-15). As for the removal of MB, the optimum initial concentration using MCM-41 and SBA-15 are 80 ppm (99.98%) and 100 ppm (99.77%), respectively.

As the concentration increases, the percentage removal of dye will decrease because the adsorption site is already concentrated with the dye [58]. This is because, at low concentrations, the ratio of the initial amount of dye molecules to the unoccupied adsorption sites was low and this causes more adsorption sites to be available hence, increasing the percentage removal. At higher concentrations, the ratio of the initial amount of dye to the unoccupied adsorption sites is high, therefore, there are less adsorption sites available hence, decreasing the percentage removal [59]. However, the removal percentage for SBA-15 increases with an increase of initial MO concentration. The adsorption capacity may increase due to the high driving force for mass transfer at a high initial dye concentration [58].

Effect of contact time

An optimum contact time can predict the mechanism of the removal process and the efficiency of the adsorbent to remove the dyes [60]. In the early stage, it is more towards the displacement of dye molecules from the bulk solution to the outer surface of the adsorbent. Consequently, at a longer contact time, the adsorption process occurs due to the interaction between the dye molecules and the adsorption sites in the inner surface of the adsorbent. Finally, the diffusion and interpenetration of the dye molecules will take place in the pores of the adsorbent [61]. In this batch of study, 0.05 g of adsorbent was used and the controlled parameters are pH and initial concentration. For MCM-41(MO), the pH and initial concentration that was chosen are pH 3 and 60 ppm. As for MCM-41 (MB), pH 7 and 80 ppm was chosen as the optimum value and for SBA-15 (MO), pH 5 was chosen with an initial concentration of 140 ppm. Lastly, for SBA-15 (MB), pH 9 and 100 ppm was chosen as the optimum values.

Adsorption isotherm

Adsorption isotherm determines whether the adsorption reaction occurs in monolayer or multilayer. It determines how the dye molecules cover the surface and internal surface of the adsorbent after the adsorption process reach equilibrium [63]. Graphs for each isotherm model are plotted to obtain linear regression correlation coefficient (R²) value that is used to define which model is suitable to explain the behavior of the adsorption occuring throughout the adsorption process. R2 value that is close to 1 is chosen. Figures 8 and 9 show the graph on the Langmuir and Freundlich isotherm model on the removal of MO and MB using MCM-41 and SBA-15, respectively. Based on the graph, the adsorption process for removal of MO (R²= 0.9742) and MB (R²= 0.9933) for MCM-41 is described as monolayer adsorption whereby the Langmuir model is best fitted for both studies [64, 65]. As for SBA-15, adsorption of MO (R²= 0.7214) is best described as the Freundlich model. Based on the previous study [66], the Langmuir model better fitting on adsorption of acidic dye, however, the result in this study does not come to an agreement. This is because the adsorbent surface during the adsorption process was heterogenous and the adsorption sites have different adsorption energy hence, causes multilayer adsorption [41]. The adsorption data on removal of MB (R²= 0.9787) using SBA-15 fits the Langmuir model [67]. Figures 8 and 9

show the graphs on the Langmuir and Freundlich isotherm model on the removal of MO and MB using MCM-41 and SBA-15, respectively.

Adsorption kinetic

There are two common kinetic models used in the kinetic study, which are pseudo-first-order or pseudo-second-order. These two kinetic models were used to investigate the mechanism of adsorption and the rate of adsorption that occurred during the adsorption process. The determination of types of kinetic model is based on the linear regression correlation coefficient, R² value

that is obtained from graphs. The R^2 value close to 1 determines the kinetic model of the adsorption process. The adsorption studies in removing MO and MB using MCM-41 and SBA-15 fit better with pseudo-second-order. This shows that the preferable mechanism of the reaction is chemisorption instead of physisorption [65, 66, 67, 68]. The graphs for t/q_t against contact time for MCM-41 and SBA-15 are shown in Figure 10 and 11, respectively.

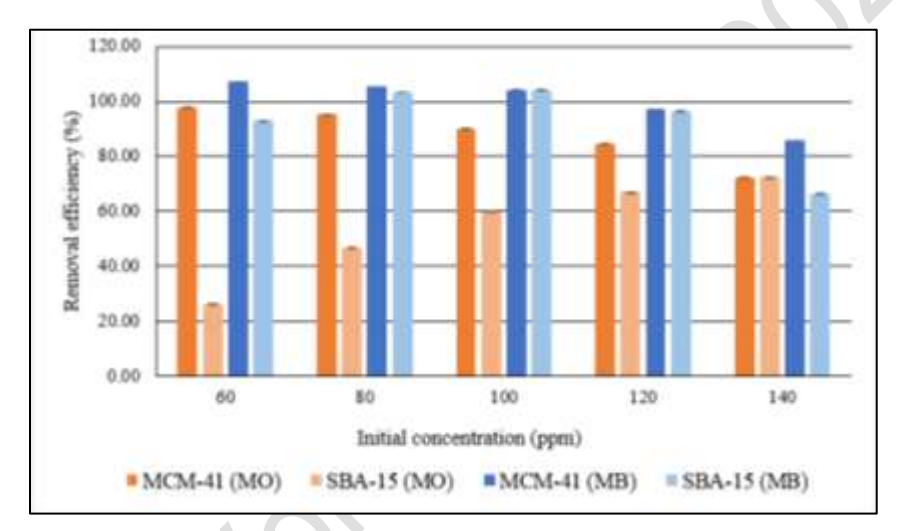


Figure 6. Percentage removal of MO and MB using MCM-41 and SBA-15 at a different range of initial concentration

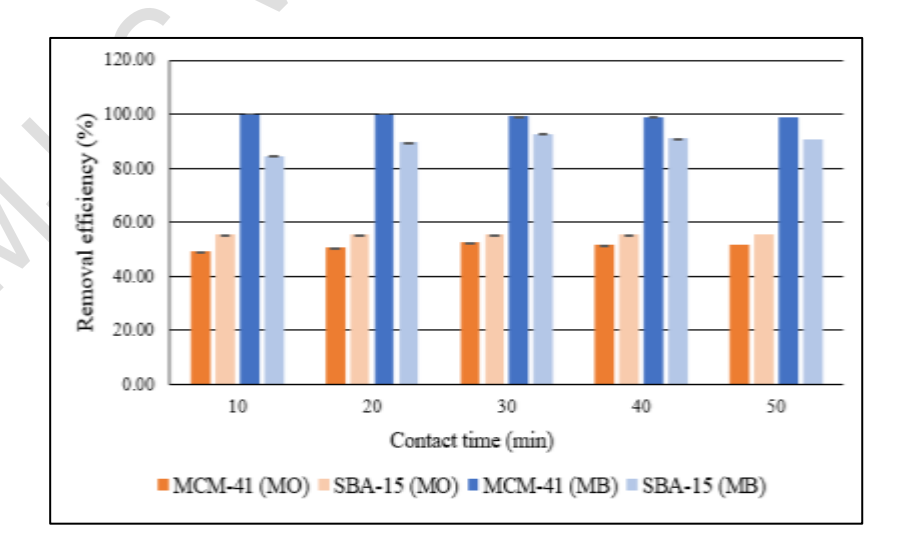


Figure 7. Percentage removal of MO and MB using MCM-41 and SBA-15 at a different range of contact time

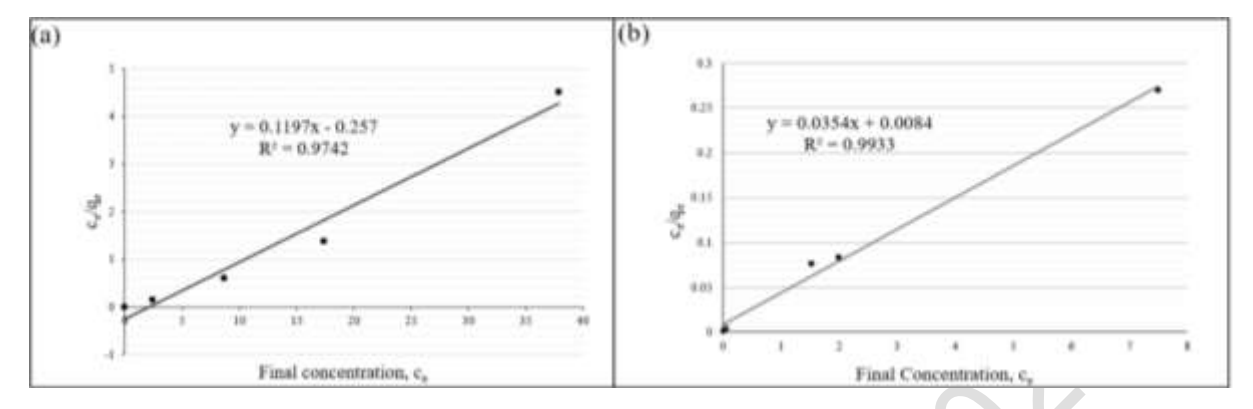


Figure 8. Langmuir adsorption isotherm on the removal of (a) MO and (b) MB using MCM-41

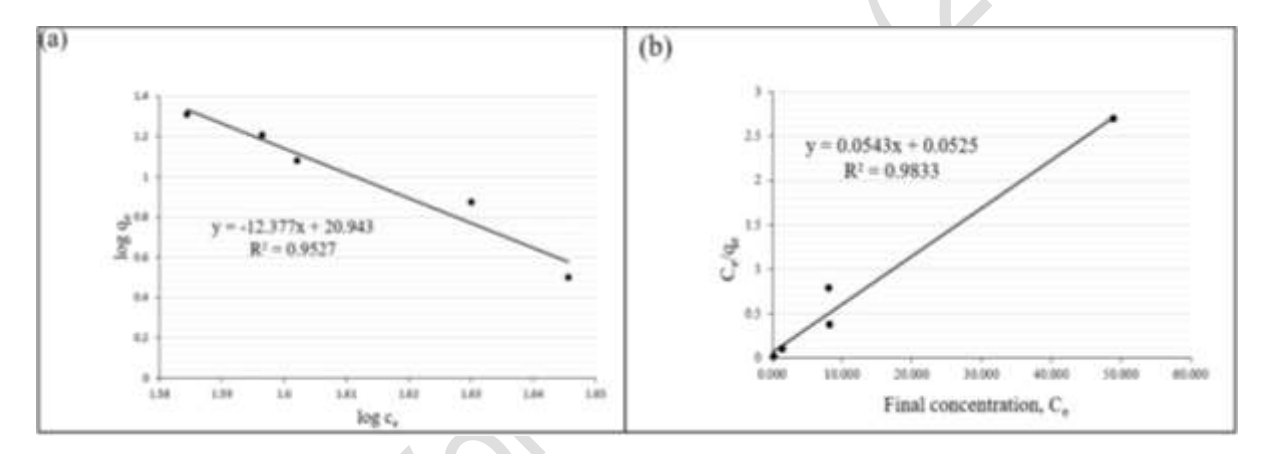


Figure 9. Freundlich adsorption isotherm on the removal of (a) MO and Langmuir isotherm on the removal of (b) MB using SBA-15

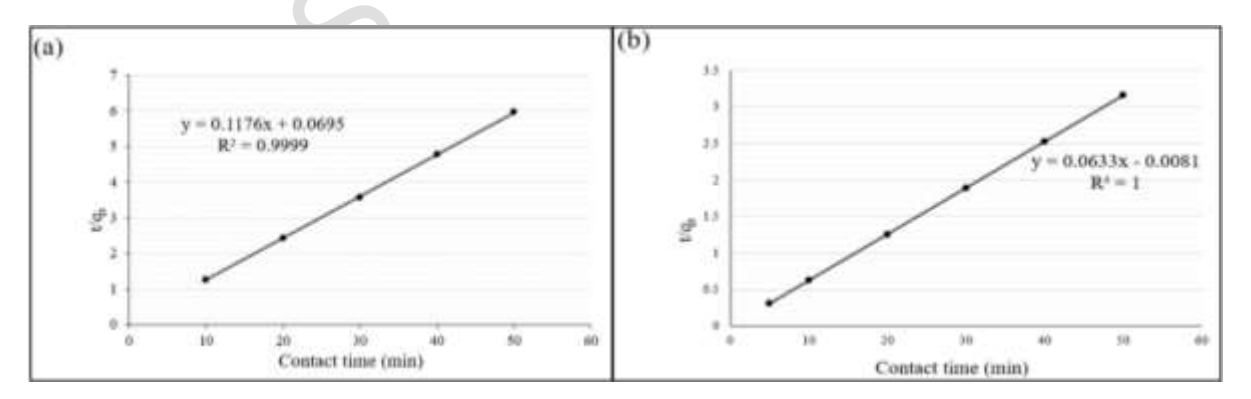


Figure 10. Pseudo-second-order for MCM-41 on removal of (a) MO and (b) MB

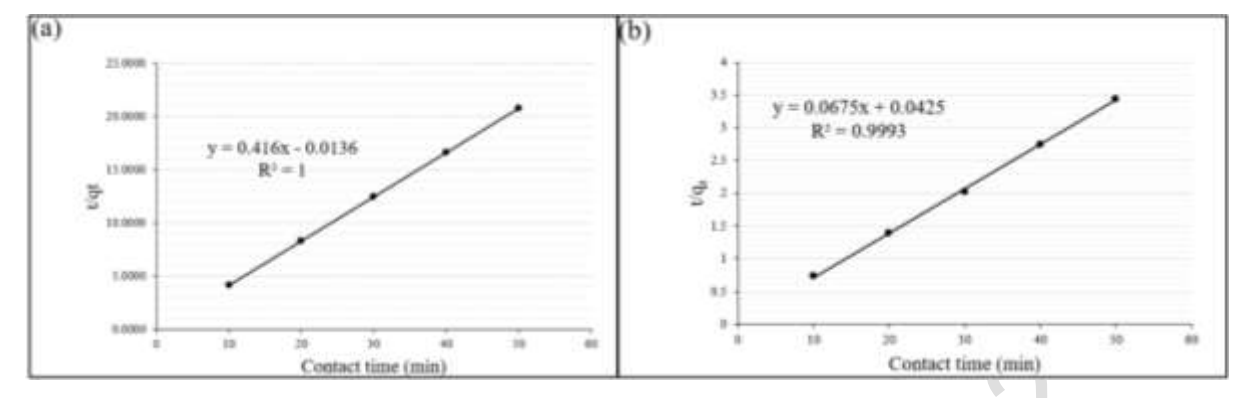


Figure 11. Pseudo-second-order for SBA-15 on removal of (a) MO and (b) MB

Comparison of dye removal efficiency

The removal efficiencies of MCM-41 and SBA-15 were compared with other types of adsorbents for removal of the MO and MB from an aqueous solution. The maximum adsorption capacity of MO and MB

dyes on different types of adsorbent are listed in Table 1. According to the table, this study showed the highest adsorption capacity for both dyes.

Table 1. Maximum adsorption capacity of MO and MB using other types of adsorbents

Mesoporous Silica Adsorbent	Dyes	pH	Maximum Adsorption Capacities, (mg/g)	References
Mesopore silica composite from rice husk with activated carbon from coconut shell	МО	2	0.470	[69]
Non-porous silica	MB	-	9.5	[70]
Green iron oxides/MCM-41	МО	4.5	1.9	[71]
Calcined magnesite	MB MO	-	0.39 0.64	[72]
Zinc metal organic frameworks	MB	-	0.75	[73]
Brazil nut shells	MB	7.0 -10.0	7.81	[74]
MCM-41	MO	3.0	4.757	This study
SBA-15	MO	5.0	20.212	This study
MCM-41	MB	7.0	16.00	This study
SBA-15	MB	11	10.45	This study

Conclusion

Mesoporous silica MCM-41 and SBA-15 with a specific surface area of 436 m²/g and 507 m²/g were applied for removal of anionic and cationic dye from an aqueous solution. At optimum conditions, the maximum adsorption capacities of MO using MCM-41 (pH = 3, initial concentration = 60 ppm, contact time = 30 minutes) and SBA-15 (pH = 5, initial concentration = 140 ppm, contact time = 40 minutes) are 4.757 mg/g and 20.212 mg/g respectively. As for the removal of MB, the maximum adsorption capacities obtained by MCM-41 (pH = 7, initial concentration = 80 ppm, contact time = 10 minutes) and SBA-15 (pH = 11, initial concentration = 100 ppm, contact time = 30 minutes) are 16.00 mg/g and 10.45 mg/g respectively. This study showed that the proposed mesoporous silicates removed a considerable amount of MB cationic dye compared to the MO anionic dye. Since cationic dyes contain positive sites, they can interact with the silanol groups and form strong hydrogen bonds for longer retention on the surface of the adsorbents. Besides that, SBA-15 removes MO better compared to MCM-41, which is due to the higher surface area and pore size. The adsorption data for the removal of MO using MCM-41 and SBA-15 fits Langmuir and Freundlich models respectively, while for the removal of MB, both adsorbents fit the Langmuir model. The adsorption kinetics of MO and MB onto MCM-41 and SBA-15 is best described as pseudo-second-order showing that the adsorption mechanism of MO and MB is chemisorption. It is concluded that MCM-41 and SBA-15 can also be used as adsorbents to efficiently remove the anionic MO and cationic MB from water.

Acknowledgement

The authors would like to thank Universiti Teknologi MARA for the facilities provided and the Technical Secretariat of the Organization for the Prohibition Chemical Weapons (OPCW) for financial aid through the research grant: 100-TNCPI/INT 16/6/2 (022/2021).

References

1. Liang, C. Z., Sun, S. P., Li, F. Y., Ong, Y. K. and Chung, T. S. (2014). Treatment of highly

- concentrated wastewater containing multiple synthetic dyes by a combined process of coagulation/flocculation and nanofiltration. *Journal of Membrane Science*, 469: 306-315.
- 2. Forster, S. V. and Christie, R. M. (2013). The sifnificance of the introduction of synthetic dyes in the mid 19th century on the democratisation of western fashion. *Journal of the International Colour Association*, 11: 1-17.
- 3. Ratna nd Padhi, B. S. (2012). Pollution due to synthetic dyes toxicity and carcinogenecity studies and remediation. *International Journal of Environmental Sciences*, 3(3): 940-947.
- 4. Kausar, A., Iqbal, M., Javed, A., Aftab, K., Nazli, Z.-i.-H., Bhatti, H. N. and Nouren, S. (2018). Dyes adsorption using clay and modified clay: A review. *Journal of Molecular Liquids*, 256: 395-407.
- 5. Lafi, R. and Hafiane, A. (2016). Removal of methyl orange (MO) from aqueous solution using cationic surfactants modified coffee waste (MCWs). *Journal of the Taiwan Institute of Chemical Engineers*, 58: 424-433.
- Elbanna, K., Sarhan, O. M., Khider, M., Elmogy, M., Abulreesh, H. H. and Shaaban, M. R. (2017). Microbiological, histological, and biochemical evidence for the adverse effects of food azo dyes on rats. *Journal of Food and Drug Analysis*, 25(3): 667-680.
- 7. Weglarz-Tomczak, E. and Gorecki, L. (2012). Azo dyes-biological activity and synthetic strategy. *Chemik Science-Technique-Market*, 66(12): 1298-1307
- 8. Percy, A. J., Moore, N. and Chipman, J. K. (1989). Formation of nuclear anomalies in rat intestine by benzidine and its biliary metabolites. *Toxicology*, 57: 217-233.
- 9. Nasuha, N., Hameed, B. H. and Din, A. T. (2010). Rejected tea as a potential low-cost adsorbent for the removal of methylene blue. *Journal of Hazardous Materials*, 175(1-3): 126-132.
- Rafatullah, M., Sulaiman, O., Hashim, R. and Ahmad, A. (2010). Adsorption of methylene blue on low-cost adsorbents: a review. *Journal of Hazardous Materials*, 177(1-3): 70-80.

- Nidheesh, P. V., Zhou, M. and Oturan, M. A. (2018). An overview on the removal of synthetic dyes from water by electrochemical advanced oxidation processes. *Chemosphere*, 197: 210-227.
- 12. Moradi, G., Zinadini, S. and Rajabi, L. (2020). Development of high flux nanofiltration membrane using para-amino benzoate ferroxane nanoparticle for enhanced antifouling behavior and dye removal. *Process Safety and Environmental Protection*, 144: 65-78.
- Hussein, T. K. and Jasim, N. A. (2021). A comparison study between chemical coagulation and electro-coagulation processes for the treatment of wastewater containing reactive blue dye. *Materials Today: Proceedings*, 42(5): 1946-1950.
- 14. Abid, M. F., Zablouk, M. A. and Abid-Alameer, A. M. (2012). Experimental study of dye removal from industrial wastewater by membrane technologies of reverse osmosis and nanofiltration. *Iranian Journal of Environmental Health Science & Engineering*, 9(1): 17.
- 15. Chen, W., Sun, F., Zhu, Z., Min, Z. and Li, W. (2014). Nanoporous SnO2 prepared by a photochemical strategy: Controlling of specific surface area and photocatalytic activity in degradation of dye pollutants. *Microporous and Mesoporous Materials*, 186: 65-72.
- 16. Yang, Z., Asoh, T. A. and Uyama, H. (2019). Removal of cationic or anionic dyes from water using ion exchange cellulose monoliths as adsorbents. *Bulletin of the Chemical Society of Japan*, 92(9): 1453-1461.
- 17. Pathania, D., Sharma, S. and Singh, P. (2013). Removal of methylene blue by adsorption onto activated carbon developed from *Ficus carica* bast. *Arabian Journal of Chemistry*, 10: S1445-S1451.
- Wang, J. and Zhuang, S. (2017). Removal of various pollutants from water and wastewater by modified chitosan adsorbents. *Critical Reviews in Environmental Science and Technology*, 47(23): 2331-2386.
- 19. Abdul Karim, S. K., Lim, S.-F., Chua, D., Shanti Faridah, S. and Puong Ling, L. (2018). Removal of crystal violet and acid green dye in aqueous

- solution using banana plant-derived sorbents. *Malaysian Journal of Analytical Sciences*, 22(1): 115-122.
- Sumari, S. M., Hamzah, Z. and Kantasamy, N. (2016). Adsorption of anionic dyes from aqueous solutions by calcined and uncalcined Mg/Al layered double hydroxide. *Malaysian Journal of Analytical Science*, 20(4), 777-792.
- 21. Wang, Y., Zhang, C., Zhao, L., Meng, G., Wu, J. and Liu, Z. (2017). Cellulose-based porous adsorbents with high capacity for methylene blue adsorption from aqueous solutions. *Fibers and Polymers*, 18(5): 891-899.
- 22. Guo, F., Jiang, X., Li, X., Jia, X., Liang, S. and Qian, L. (2020). Synthesis of MgO/Fe₃O₄ nanoparticles embedded activated carbon from biomass for high-efficient adsorption of malachite green. *Materials Chemistry and Physics*, 240: 122240.
- 23. Islam, M. A., Ahmed, M. J., Khanday, W. A., Asif, M. and Hameed, B. H. (2017). Mesoporous activated coconut shell-derived hydrochar prepared via hydrothermal carbonization-NaOH activation for methylene blue adsorption. *Journal* of Environmental Management, 203: 237-244.
- Jiang, C., Wang, X., Qin, D., Da, W., Hou, B., Hao, C. and Wu, J. (2019). Construction of magnetic lignin-based adsorbent and its adsorption properties for dyes. *Journal of Hazardous Materials*, 369: 50-61.
- Kantasamy, N. and Sumari, S. M. (2016).
 Equilibrium and thermodynamic studies of anionic dyes removal by an anionic clay-layered double hydroxide. *Malaysian Journal of Analytical Sciences*, 20(2): 358-364.
- Qu, W., He, D., Huang, H., Guo, Y., Tang, Y. and Song, R. J. (2020). Characterization of aminocrosslinked hypromellose and its adsorption characteristics for methyl orange from water. *Journal of Materials Science*, 55(17): 7268-7282.

- 27. Yang, X. J., Zhang, P., Li, P., Li, Z., Xia, W., Zhang, H., Di, Z., Wang, M., Zhang, H. and Niu, O. J. (2019).Lavered double hydroxide/polyacrylamide nanocomposite hydrogels: Green preparation, rheology and application in methyl orange removal from aqueous solution. Journal Molecular Liquids, 280: 128-134.
- 28. Wang, D., Shen, H., Guo, L., Wang, C. and Fu, F. (2016). Porous BiOBr/Bi2MoO6 heterostructures for highly selective adsorption of methylene blue. *ACS Omega*, 1(4): 566-577.
- 29. Gibson, L. T. (2014). Mesosilica materials and organic pollutant adsorption: part B removal from aqueous solution. *Chemistry Society Reviews*, 43(15): 5173-5182.
- Boukoussa, B., Hakiki, A., Moulai, S., Chikh, K., Kherroub, D. E., Bouhadjar, L., Guedal, D., Messaoudi, K., Mokthar, F. and Hamacha, R. (2018). Adsorption behaviors of cationic and anionic dyes from aqueous solution on nanocomposite polypyrrole/SBA-15. *Journal of Materials Science*, 53(10): 7372-7386.
- 31. Kresge, C. T., Leonowicz, M. E., Roth, W. J., Vartuli, J. C. and Beck, J. S. (1992). Ordered mesoporous sieves synthesised by a liquid-crystal template mechanism. *Nature*, 359: 710-712.
- 32. Björk, E. M. (2016). Synthesizing and characterizing mesoporous silica SBA-15: A hands-on laboratory experiment for undergraduates using various instrumental techniques. *Journal of Chemical Education*, 94(1): 91-94.
- 33. Sabri, A. A., Albayati, T. M. and Alazawi, R. A. (2015). Synthesis of ordered mesoporous SBA-15 and its adsorption of methylene blue. *Korean Journal of Chemical Engineering*, 32(9): 1835-1841.
- 34. Alothman, Z. (2012). A review: Fundamental aspects of silicate mesoporous materials. *Materials*, 5(12): 2874-2902.
- Xiao, X., Zhang, F., Feng, Z., Deng, S. and Wang, Y. (2015). Adsorptive removal and kinetics of methylene blue from aqueous solution using NiO/MCM-41 composite. *Physica E: Low-*

- dimensional Systems and Nanostructures, 65: 4-12.
- 36. Diagboya, P. N. E. and Dikio, E. D. (2018). Silicabased mesoporous materials; emerging designer adsorbents for aqueous pollutants removal and water treatment. *Microporous and Mesoporous Materials*, 266: 252-267.
- 37. Kamaruzaman, S., Sanagi, M. M., Endud, S., Wan Ibrahim, W. A. and Yahaya, N. (2013). MCM-41 solid phase membrane tip extraction combined with liquid chromatography for the determination of non-steroidal anti-inflammatory drugs in human urine. *Journal of Chromatography B*, 940: 59-65.
- 38. Ab Rahman, N. B., Rashid, H. M., Hassan, H. M. and Jalil, M. N. (2016). Synthesis and characterization of mesoporous silica MCM-41 and SBA-15 from power plant bottom ash. *Malaysian Journal of Analytical Sciences*, 20(3): 539-545.
- 39. Yuan, N., Cai, H., Liu, T., Huang, Q. and Zhang, X. (2019). Adsorptive removal of methylene blue from aqueous solution using coal fly ash-derived mesoporous silica material. *Adsorption Science & Technology*, 37(3-4): 333-348.
- 40. Rizzi, V., Romanazzi, F., Gubitosa, J., Fini, P., Romita, R., Agostiano, A., Petrella, A., Cosma, P. (2019). Chitosan film as eco-friendly and recyclable bio-adsorbent to remove/recover diclofenac, ketoprofen, and their mixture from wastewater. *Biomolecules*, 9(10): 571.
- 41. Rizzi, V., Gubitosa, J., Fini, P., Nuzzo, S. and Cosma, P. (2020). Amino-grafted mesoporous MCM-41 and SBA-15 recyclable adsorbents: Desert-rose-petals-like SBA-15 type as the most efficient to remove azo textile dyes and their mixture from water. Sustainable Materials and Technologies, 26: e00231.
- 42. Morsi, R. E. and Mohamed, R. S. (2018). Nanostructured mesoporous silica: influence of the preparation conditions on the physical-surface properties for efficient organic dye uptake. *Royal Society Open Science*, 5(3): 172021.

- 43. Shu, Y., Shao, Y., Wei, X., Wang, X., Sun, Q., Zhang, Q. and Li, L. (2015). Synthesis and characterization of Ni-MCM-41 for methyl blue adsorption. *Microporous and Mesoporous Materials*, 214: 88-94.
- 44. Loganathan, S., Tikmani, M. and Ghoshal, A. K. (2013). A novel pore-expanded MCM-41 for CO₂ capture: Synthesis and characterization. *Langmuir*, 29(10): 3491-3499.
- 45. He, R., Wang, Z., Tan, L., Zhong, Y., Li, W., Xing, D., Wei, C. and Tang, Y. (2018). Design and fabrication of highly ordered ion imprinted SBA-15 and MCM-41 mesoporous organosilicas for efficient removal of Ni²⁺ from different properties of wastewaters. *Microporous and Mesoporous Materials*, 257: 212-221.
- Ruthstein, S., Frydman, V., Kababya, S., Landau, M. and Goldfarb, D. (2003). Study of the formation of the mesoporous material SBA-15 by EPR spectroscopy. *The Journal of Physical Chemistry B*, 107(8): 1739-1748.
- 47. Ghorbani, F., Habibollah, Y., Mehraban, Z., Çelik, M. S., Ghoreyshi, A. A. and Anbia, M. (2013). Preparation and characterization of highly pure silica from sedge as agricultural waste and its utilization in the synthesis of mesoporous silica MCM-41. *Journal of the Taiwan Institute of Chemical Engineers*, 44(5): 821-828.
- 48. Veregue, F. R., de Lima, H. H. C., Ribeiro, S. C., Almeida, M. S., da Silva, C. T. P., Guilherme, M. R. and Rinaldi, A. W. (2020). MCM-41/chondroitin sulfate hybrid hydrogels with remarkable mechanical properties and superabsorption of methylene blue. *Carbohydrate Polymers*, 247: 116558.
- 49. Akpotu, S. O. and Moodley, B. (2018). Application of as-synthesised MCM-41 and MCM-41 wrapped with reduced graphene oxide/graphene oxide in the remediation of acetaminophen and aspirin from aqueous system. *Journal of Environmental Economics and Management*, 209: 205-215.
- Björk, E. M. (2013). Mesoporous building blocks
 synthesis and characterization of mesoporous silica particles and films. Doctoral dissertation,
 Linköping University, Sweden.

- Thommes, M., Kaneko, K., Neimark, A. V., Olivier, J. P., Rodriguez-Reinoso, F., Rouquerol, J. and Sing, K. S. W. (2015). Physisorption of gases, with special reference to the evaluation of surface area and pore size distribution (IUPAC Technical Report). Pure and Applied Chemistry, 87(9-10): 1051-1069.
- 52. Zhu, C., Xia, Y., Zai, Y., Dai, Y., Liu, X., Bian, J., Liu, Y., Liu, J. and Li, G. (2019). Adsorption and desorption behaviors of HPEI and thermoresponsive HPEI based gels on anionic and cationic dyes. *Chemical Engineering Journal*, 369: 863-873.
- 53. Alkan, M., Demirbas, O. and Dogan, M. (2004). Removal of Acid Yellow 49 from aqueous solution by adsorption. *Fresenius Environmental Bulletin*, 13(11): 1121.
- 54. Fil, B. A., Ozmetin, C. and Korkmaz, M. (2012). Cationic dye (methylene blue) removal from aqueous solution by montmorillonite. *Bulletin of the Korean Chemical Society*, 33(10): 3184-3190.
- 55. Ansari, R. and Mosayebzadeh, Z. (2010). Removal of basic dye methylene blue from aqueous solutions using sawdust and sawdust coated with polypyrrole. *Journal of the Iranian Chemical Society*, 7(2): 339-350.
- 56. Bharathi, K. S. and Ramesh, S. T. (2013). Removal of dyes using agricultural waste as low-cost adsorbents: a review. *Applied Water Science*, 3(4): 773-790.
- 57. Özdemir, Y., Doğan, M. and Alkan, M. (2006). Adsorption of cationic dyes from aqueous solutions by sepiolite. *Microporous and Mesoporous Materials*, 96(1-3): 419-427.
- Yagub, M. T., Sen, T. K., Afroze, S. and Ang, H. M. (2014). Dye and its removal from aqueous solution by adsorption: A review. Advances in Colloid and Interface Science, 209: 172-184.
- 59. Huang, R., Liu, Q., Huo, J. and Yang, B. (2017). Adsorption of methyl orange onto protonated cross-linked chitosan. *Arabian Journal of Chemistry*, 10(1): 24-32.

- 60. El-Gamal, S. M. A., Amin, M. S. and Ahmed, M. A. (2015). Removal of methyl orange and bromophenol blue dyes from aqueous solution using Sorel's cement nanoparticles. *Journal of Environmental Chemical Engineering*, 3(3): 1702-1712.
- Melo, B. C., Paulino, F. A. A., Cardoso, V. A., Pereira, A. G. B., Fajardo, A. R. and Rodrigues, F. H. A. (2018). Cellulose nanowhiskers improve the methylene blue adsorption capacity of chitosan-gpoly (acrylic acid) hydrogel. *Carbohydrate Polymers*, 181, 358–367.
- 62. Albayati, T. M., Alwan, G. M. and Mahdy, O. S. (2016). High performance methyl orange capture on magnetic nanoporous MCM-41 prepared by incipient wetness impregnation method. *Korean Journal of Chemical Engineering*, 34(1), 259–265.
- 63. Brdar, M., Šćiban, M., Takači, A. and Došenović, T. (2012). Comparison of two and three parameters adsorption isotherm for Cr(VI) onto Kraft lignin. *Chemical Engineering Journal*, 183: 108-111.
- Qin, Q., Ma, J. and Liu, K. (2009). Adsorption of anionic dyes on ammonium-functionalized MCM-41. *Journal of Hazardous Materials*, 162(1): 133-139.
- 65. Juang, L. C., Wang, C. C. and Lee, C. K. (2006). Adsorption of basic dyes onto MCM41. *Chemosphere*, 64(11): 1920-1928.
- 66. Mirzaie, M., Rashidi, A., Tayebi, H.-A. and Yazdanshenas, M. E. (2017). Removal of anionic dye from aqueous media by adsorption onto SBA-15/polyamidoamine dendrimer hybrid: Adsorption equilibrium and kinetics. *Journal of Chemical & Engineering Data*, 62(4): 1365-1376.
- 67. Bardajee, G. R., Hooshyar, Z. and Shahidi, F. E. (2015). Synthesis and characterization of a novel Schiff-base/SBA-15 nanoadsorbent for removal of methylene blue from aqueous solutions. *International Journal of Environmental Science and Technology*, 12(5): 1737-1748.
- 68. Jalil, M. N. (2011). The preparation and characterisation of mesoporous films for

- electrochemical applications. Doctoral dissertation, University of Manchester, United Kingdom.
- 69. Yusmaniar, Y., Erdawati, E., Ghifari, Y. F. and Ubit, D. P. (2020). Synthesis of mesopore silica composite from rice husk with activated carbon from coconut shell as absorbent methyl orange color adsorbent. *IOP Conference Series: Materials Science and Engineering*, 830: 032078.
- 70. Ge, S., Geng, W., He, X., Zhao, J., Zhou, B., Duan, L., Wu, Y. and Zhang, Q. (2018). Effect of framework structure, pore size and surface modification on the adsorption performance of methylene blue and Cu²⁺ in mesoporous silica. *Colloids and Surfaces A: Physicochemical and Engineering Aspects*, 539: 154-162.
- 71. Nazar de Souza, A. P., Licea, Y. E., Colaço, M. V., Senra, J. D. and Carvalho, N. M. F. (2021). Green iron oxides/amino-functionalized MCM-41 composites as adsorbent for anionic azo dye: Kinetic and isotherm studies. *Journal of Environmental Chemical Engineering*, 9(2): 105062.
- 72. Ngulube, T., Gumbo, J. R., Masindi, V. and Maity, A. (2018). Calcined magnesite as an adsorbent for cationic and anionic dyes: characterization, adsorption parameters, isotherms and kinetics study. *Heliyon*, 4(10): e00838.
- 73. Sun, C. Y., Wang, X. L., Qin, C., Jin, J. L., Su, Z. M., Huang, P. and Shao, K. Z. (2013). Solvatochromic behavior of chiral mesoporous metal-organic frameworks and their applications for sensing small molecules and separating cationic dyes. *Chemistry A European Journal*, 19(11): 3639-3645.
- 74. de Oliveira Brito, S. M., Andrade, H. M. C., Soares, L. F. and de Azevedo, R. P. (2010). Brazil nut shells as a new biosorbent to remove methylene blue and indigo carmine from aqueous solutions. *Journal of Hazardous Materials*, 174 (1-3): 84-92.